Classical Spin Liquid Instability Driven By Off-Diagonal Exchange in Strong Spin-Orbit Magnets

Ioannis Rousochatzakis and Natalia B. Perkins

Phys. Rev. Lett. **118**, 147204 — Published 5 April 2017

DOI: 10.1103/PhysRevLett.118.147204

Classical spin liquid instability driven by off-diagonal exchange in strong spin-orbit magnets

Ioannis Rousochatzakis and N. B. Perkins
School of Physics and Astronomy, University of Minnesota, Minneapolis, MN 55455, USA
(Dated: March 2, 2017)

We show that the off-diagonal exchange anisotropy drives Mott insulators with strong spin-orbit coupling to a classical spin liquid regime, characterized by an infinite number of ground states and Ising variables living on closed or open strings. Depending on the sign of the anisotropy, quantum fluctuations either fail to lift the degeneracy down to very low temperatures, or select non-coplanar magnetic states with unconventional spin correlations. The results apply to all 2D and 3D tri-coordinated materials with bond-directional anisotropy, and provide a consistent interpretation of the suppression of the x-ray magnetic circular dichroism signal reported recently for β-Li_2IrO_3 under pressure.

Introduction – The search for quantum spin liquids (QSLs) has been a central thread of correlated electron material research since their initial proposal decades ago. [1] Ideally, QSLs evade magnetic order down to zero temperature and harbor a remarkable set of collective phenomena, including topological ground-state degeneracy, long-range entanglement, and fractionalized excitations. [2–4] While the long activity on frustrated Mott insulators with $3d$ ions has lead to several candidate QSLs with dominant isotropic interactions, [3] a certain class of $4d$ and $5d$ materials, the so-called Jackeli-Khaliullin Kitaev (JKK) systems, [5–10] with strong spin orbit coupling (SOC) and dominant anisotropic interactions has emerged in recent years as another prominent playground for QSLs. [11] By now, several two- (2D) and three-dimensional (3D) materials have been identified in the JKK class, all described by pseudo-spin $J_{\rm eff}=1/2$ Kramer's doublets. Most notably, the layered A_2IrO_3 (A=Na,Li) [12–18] and α-$RuCl_3$, [19–24] and the 3D Iridates (β,γ)-Li_2IrO_3, [25–28] all proximate to exactly solvable Kitaev QSL's. [5, 9, 29]

The key ingredients for the desired degree of frustration in the JKK systems is the three-fold coordination and the compass-like, nearest-neighbor (NN) Ising interactions along bond-dependent quantization axes. [7, 30–39] While this so-called Kitaev anisotropy is the dominant interaction, all JKK materials show magnetic order at sufficiently low temperatures, [12–28] consistent with predictions that Kitaev QSLs are fragile against perturbations. [7, 8, 30, 40–44]

Nevertheless, the aspiration for spin liquid physics in JKK systems still stands. The new experimental direction is to use external perturbations, such as magnetic field, [45] chemical substitution, [46] and pressure. [28] For β-Li_2IrO_3, for example, x-ray magnetic circular dichroism (XMCD) experiments show a strong reduction of the signal with pressure, and a complete suppression around 2 GPa. [28] Since the system remains insulating under pressure, the authors suggest that the system is driven into a spin-liquid regime, and naturally the Kitaev QSL is the first suspect. Surprisingly, however, according to two independent *ab initio* studies, [39, 47] pressure pushes the system further away from the ideal Kitaev model, and the interaction becoming increasingly relevant is the symmetric off-diagonal exchange Γ. [30–32, 37, 38, 42]

Motivated by these reports, we set out to investigate the physics of the JKK systems in the region where Γ is the dominant coupling. Remarkably, the qualitative results are shared by all 2D and 3D JKK systems. The Γ coupling drives these systems to a classical spin liquid regime, characterized by an infinite number of ground states. This is consistent with the report that the spin correlation length becomes extremely small as we go into the large Γ regime. [32] The infinite degeneracy is not accidental but arises from an infinite number of zero- (0D) and one-dimensional (1D) gauge symmetries that exist only for classical spins. For quantum spins, the degeneracy is eventually lifted by the order-by-disorder mechanism at an energy scale which depends strongly on the sign of Γ. For $\Gamma>0$, the leading quantum fluctuations fail to remove the frustration, leading to a 'cooperative paramagnet' down to very low temperatures. For $\Gamma<0$, fluctuations select a non-coplanar state with vanishing total moment. Both scenarios are consistent with the XMCD data, although the latter might be more relevant for β-Li_2IrO_3, according to *ab initio* studies. [39, 47]

Model – The JKK systems have three types of NN bonds, $\alpha=\{x,y,z\}$, shown as

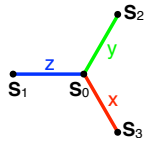

(1)

where $\mathbf{S}_i$ denotes the pseudospin 1/2 at site i. The Hamiltonian describing the off-diagonal exchange reads

$$\mathcal{H}=\pm\Gamma\sum_{\langle ij\rangle\in\text{'x'}}(S_i^yS_j^z+S_i^zS_j^x)\pm\Gamma\sum_{\langle ij\rangle\in\text{'y'}}(S_i^zS_j^x+S_i^xS_j^z)$$
$$+\Gamma\sum_{\langle ij\rangle\in\text{'z'}}(S_i^xS_j^y+S_i^yS_j^x), \qquad (2)$$

where $\langle ij\rangle$ denotes NN sites, and $\pm$ accounts for the sign modulation of the couplings on x- and y-bonds in the 3D systems. [48] For the 2D case all bonds have the plus sign.

Classical limit – Let us consider the classical limit where $\mathbf{S}_i$ are vectors of length S, and begin with the 2D honeycomb case. The highly frustrated nature of this model is first revealed by the fact that the lowest eigenvalue of the 6×6 interaction matrix $\mathbf{\Lambda_k}$ in momentum space [49] is completely flat. In fact, this holds for all six bands, with $\lambda_1=-|\Gamma|$, $\lambda_2=\lambda_3=-|\Gamma|/2$, $\lambda_4=\lambda_5=|\Gamma|/2$, and $\lambda_6=|\Gamma|$, see Fig.1.

To understand the nature of the ground states and why there is an infinite number of them, we search for states that saturate the lower bound of the energy per site λ_1S^2. [49] Consider a pair of spins, say $\mathbf{S}_0$ and $\mathbf{S}_1$ of (1), which interact via

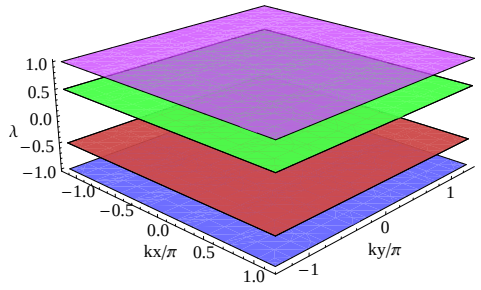

FIG. 1. Spectrum $\lambda_{1-6}/|\Gamma|$ of the matrix $\mathbf{\Lambda_k}$ entering the Fourier transform of the classical energy, see Supplementary material. [49]

$\Gamma\,(S_0^x S_1^y + S_0^y S_1^x)$. If these spins were isolated from the rest, then their energy would be minimized by placing the spins on the xy-plane with $S_1^x = \zeta S_0^y$, $S_1^y = \zeta S_0^x$, $\zeta = -\mathrm{sgn}(\Gamma)$. Similarly, for the x-bond of (1), we would get $S_3^y = \zeta S_0^z$, $S_3^z = \zeta S_0^y$, and for the y-bond of (1), $S_2^x = \zeta S_0^z$, $S_2^z = \zeta S_0^x$. Returning to the lattice problem, the idea is to require that the two components involved in each Γ term satisfy the respective relations above, without specifying the third component for the moment. This is done as follows: (i) We choose a direction for the central spin of (1) and parametrize it as

$$\mathbf{S}_0 = (\eta_1 a, \eta_2 b, \eta_3 c), \tag{3}$$

where $a = |S_0^x|$, $b = |S_0^y|$, $c = |S_0^z|$, $\eta_1 = \mathrm{sgn}(S_0^x)$, $\eta_2 = \mathrm{sgn}(S_0^y)$ and $\eta_3 = \mathrm{sgn}(S_0^z)$. Then, (ii) we fix two components of the three neighbors as:

$$\begin{gathered}\mathbf{S}_1 = (\zeta\eta_2 b, \zeta\eta_1 a, S_1^z), \quad \mathbf{S}_2 = (\zeta\eta_3 c, S_2^y, \zeta\eta_1 a), \\ \mathbf{S}_3 = (S_3^x, \zeta\eta_3 c, \zeta\eta_2 b).\end{gathered} \tag{4}$$

Then, (iii) we fix accordingly two components of the neighbors of $\mathbf{S}_{1,2,3}$, etc, until we cover the whole lattice. The total energy of the generated configurations saturates the lower energy bound, and are therefore ground states. Indeed, the energy contribution from the cluster (1) is $E_{\hexagon} = -2(a^2 + b^2 + c^2)|\Gamma| = -2|\Gamma|S^2$, and this holds for any such cluster in the lattice. Since each bond is shared by two sites, the total energy per site is $E/N = -|\Gamma|S^2$, which saturates the lower bound.

Now, the reason why there are infinite ground states lies in the freedom to choose the third component of the spins, i.e., S_1^z, S_2^y, S_3^x, etc. Imposing the spin length constraint shows that this freedom is associated with the overall signs:

$$S_1^z = \zeta\eta_4 c, \; S_2^y = \zeta\eta_5 b, \; S_3^x = \zeta\eta_6 a, \tag{5}$$

where $\eta_i = \pm 1$ are Ising variables. The choice of signs in front of the η's give the simplest representation of the state as we see below, but is otherwise arbitrary. To see how many independent η's exist, we look closely what happens around the central cluster (1), see Fig. 2. We see that each η_i appears only around a single hexagon, i.e. we can label the states by assigning the η's to the hexagons. This parametrization in terms of *local* Ising variables gives a total of $2^{N/2}$ states for fixed $\{a, b, c\}$. Note that if two (one) of $\{a, b, c\}$ vanish then 2/3 (1/3) of the η's are idle and we get $2^{N/6}$ ($2^{N/3}$) states instead. On top, there is the degeneracy associated to $\{a, b, c\}$.

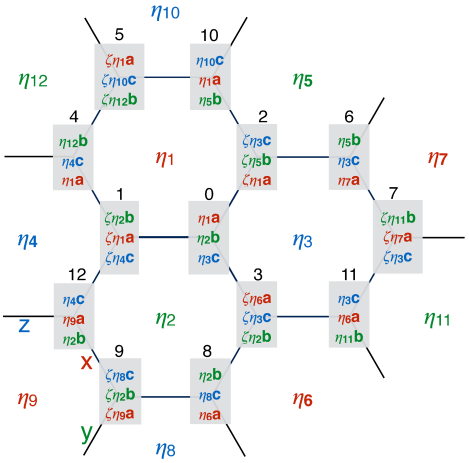

FIG. 2. Classical ground states of the Γ model on the 2D honeycomb lattice, where $a^2 + b^2 + c^2 = S^2$ and $\eta_i = \pm 1$.

The η-parametrization reveals that the local zero-energy modes responsible for the extensive degeneracy correspond to flipping one particular component for each of the six spins of a hexagon. For the η_1 hexagon of Fig. (2), for example, the zero mode amounts to flipping the signs of S_0^x, S_1^y, S_4^z, S_5^x, S_{10}^y, and S_2^z. This operation is in fact a symmetry of the classical Hamiltonian, so the degeneracy associated with the η's is not accidental but symmetry related. Inspecting the form of the Γ terms, these symmetries involve strings of alternating x-y-z bonds which happen to be hexagons in the 2D honeycomb case. We shall come back to this for the 3D cases below.

Another key aspect of the η variables is that they split into three inequivalent types that occupy the vertices of three interpenetrating triangular sublattices A, B and C (red, green and blue in Fig. 2). Type-A (resp. B, C) variables appear together with a (resp. b, c). This structure is reflected directly in the so-called fluxes $\{W_h\}$, known from the quantum Kitaev model. [5] Indeed, from Fig. 2:

$$W_{h\in A} = W_{\eta_1} = S_0^x S_1^y S_4^z S_5^x S_{10}^y S_2^z / S^6 = \zeta\tilde{a}^6, \tag{6}$$

$$W_{h\in B} = W_{\eta_2} = S_8^x S_9^y S_{12}^z S_1^x S_0^y S_3^z / S^6 = \zeta\tilde{b}^6, \tag{7}$$

$$W_{h\in C} = W_{\eta_3} = S_{11}^x S_3^y S_0^z S_2^x S_6^y S_7^z / S^6 = \zeta\tilde{c}^6, \tag{8}$$

where $\tilde{a} = a/S$, $\tilde{b} = b/S$ and $\tilde{c} = c/S$. [50] The most striking manifestation of the three-sublattice structure of the η's, however, appears when we include quantum fluctuations below.

The above steps can be repeated for both β-Li_2IrO_3 and γ-Li_2IrO_3, see Fig. 3. There are again infinite ground states characterized by Ising variables η of three types, as in 2D. There is however one qualitative difference in the nature of the zero-energy modes which stems from the way alternating x-y-z bonds propagate in the lattice. In β-Li_2IrO_3, they form infinite strings, so all η's are *nonlocal* [see e.g. the η_2 string in Fig. 3 (a)] and the degeneracy is sub-extensive. In γ-Li_2IrO_3, the alternating x-y-z bonds form either closed hexagons or infinite strings. Hence, some η's are local (giving an extensive degeneracy), like η_1, η_{12}, η_2, η_8, η_5 and η_9 in Fig. 3 (b), but the rest live on open strings, like η_3.

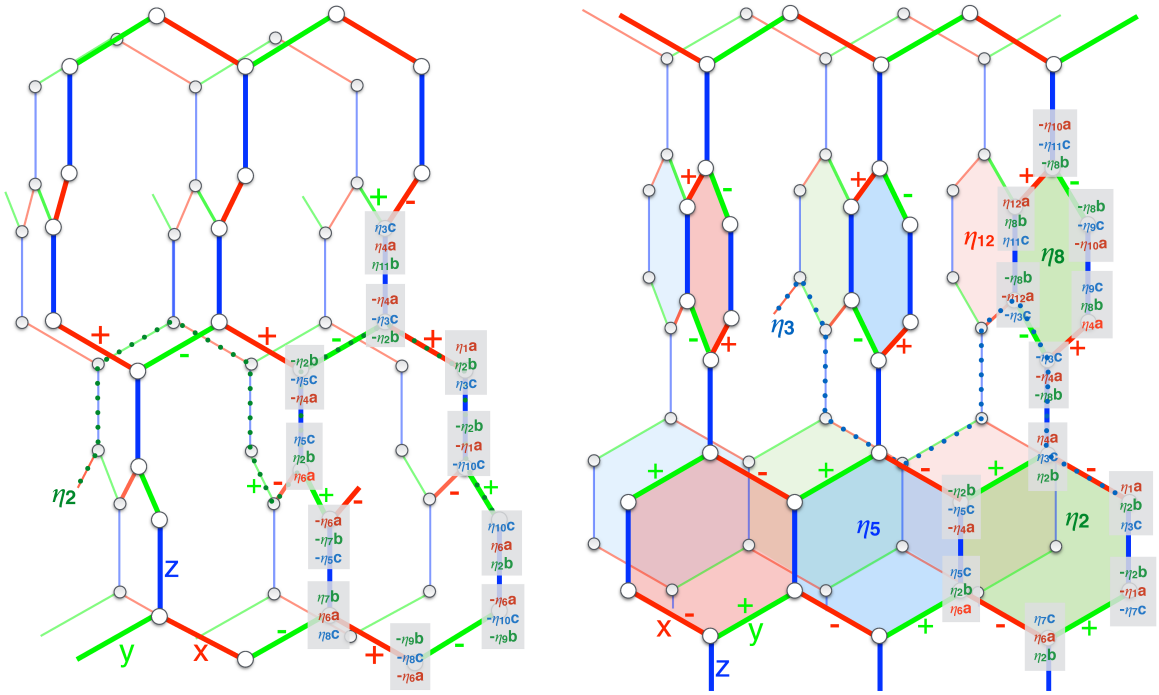

FIG. 3. Classical ground states of the Γ model on β-Li_2IrO_3 (a) and γ-Li_2IrO_3 (b), for $\Gamma>0$. The $\pm$ signs labeling the x or y bonds denote the signs of the associated Γ coupling relative to that on the z bonds. [48] The dotted strings show the open strings where η_2 (a) and η_3 (b) live.

Quantum order-by-disorder – The 0D and 1D gauge symmetries that are responsible for the zero-energy modes are very common in compass-like models and act to suppress local order by virtue of a generalized Elitzur's theorem. [51–53] Here, however, these symmetries exist only for classical spins, because they involve time reversal and affect only part of the system (a hexagon or an open string). For quantum spins the degeneracy is lifted and local order is still possible. This leads us to the important question of order-by-disorder, which we address here by real space perturbation theory (RSPT). [54–57] In this approach, one introduces local axes $\mathbf{e}_i^z$ along the classical spin directions, and then splits $\mathcal{H}$ into a diagonal part $\mathcal{H}_0 = h\sum_i (S-\mathbf{S}_i\cdot\mathbf{e}_i^z)$, describing fluctuations in the local field $h=2|\Gamma|S$, and a perturbation $\mathcal{V}=\mathcal{H}-\mathcal{H}_0$, which couples fluctuations on different sites. [49]

It turns out that the physics can be captured already by the leading, short-wavelength corrections from second-order perturbation theory. The three types of bonds, say $(\mathbf{S}_0,\mathbf{S}_3)$, $(\mathbf{S}_0,\mathbf{S}_2)$ and $(\mathbf{S}_0,\mathbf{S}_1)$ of Fig. (2), give (disregarding constants):

$$\begin{aligned}\delta E_{03} &= (\Gamma S\tilde{a}^2/8)\eta_1\eta_6 - |\Gamma|S\tilde{a}^4/16,\\ \delta E_{02} &= (\Gamma S\tilde{b}^2/8)\eta_2\eta_5 - |\Gamma|S\tilde{b}^4/16,\\ \delta E_{01} &= (\Gamma S\tilde{c}^2/8)\eta_3\eta_4 - |\Gamma|S\tilde{c}^4/16.\end{aligned} \tag{9}$$

These expressions give two important insights:

(i) Different types of η's do not couple. This is a consequence of three gauge-like symmetries which flip the sign of all η's of a given type [49]; Different η types eventually couple in fourth order, but the coupling is much smaller, see below. Each η-sublattice then is described by Ising couplings $J_A=\Gamma S\tilde{a}^2/8$, $J_B=\Gamma S\tilde{b}^2/8$, or $J_C=\Gamma S\tilde{c}^2/8$. Remarkably, when $\Gamma>0$, these models are highly frustrated for all 2D and 3D cases. In 2D, each η-sublattice is described by a triangular Ising antiferromagnet (AF), the prototype of classical spin liquids. [58] For the hyper-honeycomb, the frustration arises again from AF η-triangles, like $\{\eta_1,\eta_4,\eta_6\}$ or $\{\eta_2,\eta_7,\eta_9\}$ or $\{\eta_5,\eta_8,\eta_{10}\}$ of Fig. 3 (a), which form at the length-ten loops of the lattice, where open strings pass nearby. The same happens for the nonlocal η's in the stripy-honeycomb, where two effective triangles such as $\{\eta_1,\eta_4,\eta_6\}$ and $\{\eta_3,\eta_5,\eta_7\}$ in Fig. 3 (b), are formed at a hexagon (η_2) of the complementary color. At the same time, the local variables form 1D AF chains (formed by hexagons), and there is also a frustrating coupling between local and nonlocal η's. So, in all cases, there is strong frustration within each η-sublattice when $\Gamma>0$.

(ii) Irrespective of the ground state of each η-sublattice, the dependence of the total energy on $\{a,b,c\}$ via J_A, J_B and J_C drops out because the sublattices have identical $\langle\eta\eta'\rangle$ correlations and because $a^2+b^2+c^2=S^2$. However, the second terms of Eq. (9) give a fourth-order cubic anisotropy,

$$E_{\rm ani}/N = -\frac{|\Gamma|S}{32}(\tilde{a}^4+\tilde{b}^4+\tilde{c}^4), \tag{10}$$

which is the leading mechanism to lift the degeneracy associated to $\{a,b,c\}$. Here, $E_{\rm ani}$ is minimized when $\{\tilde{a},\tilde{b},\tilde{c}\}=\{1,0,0\}$, $\{0,1,0\}$ or $\{0,0,1\}$. Then, 2/3 of the η's become idle and only the behavior of the remaining 1/3 has to be understood.

For $\Gamma>0$, the systems remain highly frustrated even well below the scale set by $E_{\rm ani}$. Residual corrections eventually

stabilize some order. In 2D, for example, tunneling loop processes give rise to an XYZ model and a peculiar state with two orders, one magnetic and one nematic. [59]

For $\Gamma<0$, the systems order magnetically below a scale set by $E_{\rm ani}$. The order corresponds to a FM alignment of η's of one type (the others become idle). In terms of spins, this is a multi-sublattice non-coplanar state, with spins pointing along the cubic axes. The 2D honeycomb has three spin sublattices and a finite moment along $\langle 111\rangle$, while for 3D we get six sublattices due to $\pm$ signs in Eq. (2). So, the ordered state of the 3D systems has zero total moment.

Higher-order terms – To highlight the unimportance of higher-order corrections we report here the fourth-order RSPT corrections on the connected cluster (1), for the most quantum $S=1/2$ case. [49] The correction to J_A is $\delta J_A = \frac{\Gamma}{768}(-14\tilde{a}^2+33\tilde{a}^4-25\tilde{a}^6+23\tilde{a}^2\tilde{b}^2\tilde{c}^2)$, and similarly for δJ_B and δJ_C by cyclic permuting $\{\tilde{a},\tilde{b},\tilde{c}\}$. These corrections are very small (at maximum they are only $1/8$ of the second-order couplings). Next, the correction to $E_{\rm ani}$ is $\delta E_{\rm ani} = \frac{-|\Gamma|}{3072}[15(\tilde{a}^4+\tilde{b}^4+\tilde{c}^4)+95\tilde{a}^2\tilde{b}^2\tilde{c}^2-22(\tilde{a}^8+\tilde{b}^8+\tilde{c}^8)]$. The second and third terms do not alter the physics, i.e., the energy is again minimized for $\{\tilde{a},\tilde{b},\tilde{c}\}$ along the cubic axes. Finally, there is a coupling between two η-types, $J_{AB}(\eta_1\eta_6)(\eta_2\eta_5)$, where $J_{AB}=\frac{7|\Gamma|}{384}\tilde{a}^2\tilde{b}^2$, etc. These terms favor also $\{\tilde{a},\tilde{b},\tilde{c}\}$ along the cubic axes. Altogether then, the second-order terms give an excellent description of the order-by-disorder physics.

Role of perturbations – At the mean-field level, the infinite degeneracy is immediately lifted by perturbations, such as NN and next-NN Kitaev (K_1 and K_2 [59]), or NN exchange (J_1). [32] The phase diagrams of Refs. [32, 60] show, for example, four states emerging from the Γ point as we include K_1 and J_1. These states are special members of the infinite manifold described above, see also [49]. This picture changes at the quantum level. Such tetra-critical points will be replaced by a finite window that is still governed by the physics of the Γ point. The reason is that quantum energy corrections scale as ΓS, while the lifting at the mean-field level involves scales like K_1S^2 or J_1S^2. This leaves a finite region $\Gamma \gtrsim \xi K_1 S$ or $\xi J_1 S$, where the physics of the Γ point survives. The numerical prefactor ξ depends on the JKK system and the perturbations. We can foresee, however, that the highly frustrated physics of the positive Γ model should be more stable on the ferromagnet K_1 side, because K_1 acts to renormalize J_A, J_B and J_C by $-K_1S^2\tilde{a}^2$, $-K_1S^2\tilde{b}^2$ and $-K_1S^2\tilde{c}^2$, respectively. This is important because K_1 is FM in all JKK materials.

Discussion – Our predictions are consistent with the XMCD data in β-Li_2IrO_3. [28] At ambient pressure, β-Li_2IrO_3 shows an incommensurate order which is very close to a partially polarized state. [28] The *ab initio* studies [39, 47] show that $|\Gamma|$, which is already appreciable at ambient pressure, increases by 10-15 % at 2 GPa, while $|K_1|$ drops by a remarkable 40-50 %. Clearly then, the system departs quickly from the vicinity of the partially polarized state, toward the classical manifold of the Γ model, and eventually orders either at a very small energy scale if $\Gamma>0$, or at the scale $E_{\rm ani}$ if $\Gamma<0$. Either way, one expects a strong suppression of the field-induced ferromagnetic moments. According to *ab initio* studies [39, 47] and fits to experiments, [48] Γ is negative, which would mean that the system orders in the above non-coplanar state. This can be confirmed e.g., by NMR or μSR.

The broader perspective of this study is that, besides the well-known Kitaev QSL, Mott insulators with strong spin-orbit coupling and bond-dependent interactions host yet another exotic correlated regime. Remarkably, the key predictions are common for all available JKK materials, providing a distinct platform for exploring this direction.

We thank A. Tsirlin, T. Takayama, R. Yadav, L. Hozoi, J. van den Brink, C. Batista, Y. Sizyuk, J. Reuther, R. Coldea, and Y. B. Kim for fruitful discussions, and acknowledge support from NSF Grant No. DMR-1511768. IR acknowledges the hospitality of MPI-PKS of Dresden where part of this work was done, and NP acknowledges the hospitality of Aspen Center for Physics and NSF GRANT No. PHY-1066293.

[1] P. Anderson, Materials Research Bulletin **8**, 153 (1973).
[2] *Introduction to Frustrated Magnetism: Materials, Experiments, Theory* (Springer Series in Solid-State Sciences, Berlin, 2011).
[3] L. Balents, Nature **464**, 199 (2010).
[4] L. Savary and L. Balents, arXiv:1601.03742 (2016).
[5] A. Kitaev, Annals of Physics **321**, 2 (2006).
[6] G. Jackeli and G. Khaliullin, Phys. Rev. Lett. **102**, 017205 (2009).
[7] J. Chaloupka, G. Jackeli, and G. Khaliullin, Phys. Rev. Lett. **105**, 027204 (2010).
[8] J. Chaloupka, G. Jackeli, and G. Khaliullin, Phys. Rev. Lett. **110**, 097204 (2013).
[9] S. Mandal and N. Surendran, Phys. Rev. B **79**, 024426 (2009).
[10] K. O'Brien, M. Hermanns, and S. Trebst, Phys. Rev. B **93**, 085101 (2016).
[11] W. Witczak-Krempa, G. Chen, Y. B. Kim, and L. Balents, Annual Review of Condensed Matter Physics **5**, 57 (2014).
[12] Y. Singh and P. Gegenwart, Phys. Rev. B **82**, 064412 (2010).
[13] Y. Singh, S. Manni, J. Reuther, T. Berlijn, R. Thomale, W. Ku, S. Trebst, and P. Gegenwart, Phys. Rev. Lett. **108**, 127203 (2012).
[14] X. Liu, T. Berlijn, W.-G. Yin, W. Ku, A. Tsvelik, Y.-J. Kim, H. Gretarsson, Y. Singh, P. Gegenwart, and J. P. Hill, Phys. Rev. B **83**, 220403 (2011).
[15] S. K. Choi, R. Coldea, A. N. Kolmogorov, T. Lancaster, I. I. Mazin, S. J. Blundell, P. G. Radaelli, Y. Singh, P. Gegenwart, K. R. Choi, S.-W. Cheong, P. J. Baker, C. Stock, and J. Taylor, Phys. Rev. Lett. **108**, 127204 (2012).
[16] F. Ye, S. Chi, H. Cao, B. C. Chakoumakos, J. A. Fernandez-Baca, R. Custelcean, T. F. Qi, O. B. Korneta, and G. Cao, Phys. Rev. B **85**, 180403 (2012).
[17] S. Hwan Chun, J.-W. Kim, J. Kim, H. Zheng, C. C. Stoumpos, C. D. Malliakas, J. F. Mitchell, K. Mehlawat, , Y. Singh, Y. Choi, T. Gog, A. Al-Zein, M. M. Sala, M. Krisch, J. Chaloupka, G. Jackeli, G. Khaliullin, and B. J. Kim, Nat Phys **10**, 1038 (2015).

[18] S. C. Williams, R. D. Johnson, F. Freund, S. Choi, A. Jesche, I. Kimchi, S. Manni, A. Bombardi, P. Manuel, P. Gegenwart, and R. Coldea, Phys. Rev. B **93**, 195158 (2016).

[19] K. W. Plumb, J. P. Clancy, L. J. Sandilands, V. V. Shankar, Y. F. Hu, K. S. Burch, H.-Y. Kee, and Y.-J. Kim, Phys. Rev. B **90**, 041112 (2014).

[20] J. A. Sears, M. Songvilay, K. W. Plumb, J. P. Clancy, Y. Qiu, Y. Zhao, D. Parshall, and Y.-J. Kim, Phys. Rev. B **91**, 144420 (2015).

[21] Y. Kubota, H. Tanaka, T. Ono, Y. Narumi, and K. Kindo, Phys. Rev. B **91**, 094422 (2015).

[22] M. Majumder, M. Schmidt, H. Rosner, A. A. Tsirlin, H. Yasuoka, and M. Baenitz, Phys. Rev. B **91**, 180401 (2015).

[23] A. Banerjee, C. Bridges, J.-Q. Yan, A. Aczel, L. Li, M. Stone, G. Granroth, M. Lumsden, Y. Yiu, J. Knolle, *et al.*, Nature materials (2016), 10.1038/nmat4604.

[24] R. D. Johnson, S. C. Williams, A. A. Haghighirad, J. Singleton, V. Zapf, P. Manuel, I. I. Mazin, Y. Li, H. O. Jeschke, R. Valentí, and R. Coldea, Phys. Rev. B **92**, 235119 (2015).

[25] A. Biffin, R. D. Johnson, S. Choi, F. Freund, S. Manni, A. Bombardi, P. Manuel, P. Gegenwart, and R. Coldea, Phys. Rev. B **90**, 205116 (2014).

[26] A. Biffin, R. D. Johnson, I. Kimchi, R. Morris, A. Bombardi, J. G. Analytis, A. Vishwanath, and R. Coldea, Phys. Rev. Lett. **113**, 197201 (2014).

[27] K. Modic, T. E. Smidt, I. Kimchi, N. P. Breznay, A. Biffin, S. Choi, R. D. Johnson, R. Coldea, P. Watkins-Curry, G. T. McCandess, *et al.*, Nature communications **5** (2014), 10.1038/ncomms5203.

[28] T. Takayama, A. Kato, R. Dinnebier, J. Nuss, H. Kono, L. S. I. Veiga, G. Fabbris, D. Haskel, and H. Takagi, Phys. Rev. Lett. **114**, 077202 (2015).

[29] I. Kimchi, J. G. Analytis, and A. Vishwanath, Phys. Rev. B **90**, 205126 (2014).

[30] V. M. Katukuri, S. Nishimoto, V. Yushankhai, A. Stoyanova, H. Kandpal, S. Choi, R. Coldea, I. Rousochatzakis, L. Hozoi, and J. van den Brink, New J. Phys. **16**, 013056 (2014).

[31] Y. Sizyuk, C. Price, P. Wölfle, and N. B. Perkins, Phys. Rev. B **90**, 155126 (2014).

[32] J. G. Rau, E. K.-H. Lee, and H.-Y. Kee, Phys. Rev. Lett. **112**, 077204 (2014).

[33] V. V. Shankar, H.-S. Kim, and H.-Y. Kee, arXiv:1411.6623 (2014).

[34] K. Foyevtsova, H. O. Jeschke, I. I. Mazin, D. I. Khomskii, and R. Valentí, Phys. Rev. B **88**, 035107 (2013).

[35] Y. Yamaji, Y. Nomura, M. Kurita, R. Arita, and M. Imada, Phys. Rev. Lett. **113**, 107201 (2014).

[36] H.-S. Kim, E. K.-H. Lee, and Y. B. Kim, Europhys. Lett. **112**, 67004 (2015).

[37] S. M. Winter, Y. Li, H. O. Jeschke, and R. Valentí, Phys. Rev. B **93**, 214431 (2016).

[38] H.-S. Kim and H.-Y. Kee, Phys. Rev. B **93**, 155143 (2016).

[39] H.-S. Kim, Y. B. Kim, and H.-Y. Kee, arXiv:1608.04741 (2016).

[40] R. Schaffer, S. Bhattacharjee, and Y. B. Kim, Phys. Rev. B **86**, 224417 (2012).

[41] E. K.-H. Lee, R. Schaffer, S. Bhattacharjee, and Y. B. Kim, Phys. Rev. B **89**, 045117 (2014).

[42] S. Nishimoto, V. M. Katukuri, V. Yushankhai, H. Stoll, U. K. Roessler, L. Hozoi, I. Rousochatzakis, and J. van den Brink, Nat Commun **7** (2016), 10.1038/ncomms10273.

[43] V. M. Katukuri, N. Satoshi, I. Rousochatzakis, H. Stoll, J. van den Brink, and L. Hozoi, Sci Rep (2015), 10.1038/srep14718.

[44] I. Rousochatzakis, J. Reuther, R. Thomale, S. Rachel, and N. B. Perkins, Phys. Rev. X **5**, 041035 (2015).

[45] B. Büchner, Talk at International FSB Conference on Frustration and Topology, Kloster Nimbschen, Germany (2016).

[46] H. Takagi, Talk at International Conference on Highly Frustrated Magnetism, Taipei, Taiwan (2016).

[47] R. Yadav, L. Hozoi, and A. Tsirlin, Private communication.

[48] E. K.-H. Lee, J. G. Rau, and Y. B. Kim, Phys. Rev. B **93**, 184420 (2016).

[49] See Supplemental material at $\cdots$, which includes [61], for auxiliary information on: i) the form of the interaction matrix $\mathbf{\Lambda_k}$, ii) some special members of the classical ground state manifold, iii) the symmetries of the quantum model, and iv) technical details and additional RSPT expressions for general S.

[50] Note that here, in contrast to the Kitaev model, the fluxes are not conserved quantities, and so they cannot be fixed independently from each other.

[51] C. D. Batista and Z. Nussinov, Phys. Rev. B **72**, 045137 (2005).

[52] Z. Nussinov, C. D. Batista, and E. Fradkin, Int. J. Mod. Phys. B **20**, 5239 (2006).

[53] Z. Nussinov and J. van den Brink, Rev. Mod. Phys. **87**, 1 (2015).

[54] P.-A. Lindgård, Phys. Rev. Lett. **61**, 629 (1988).

[55] M. W. Long, Journal of Physics: Condensed Matter **1**, 2857 (1989).

[56] M. T. Heinilä and A. S. Oja, Phys. Rev. B **48**, 7227 (1993).

[57] A. L. Chernyshev and M. E. Zhitomirsky, Phys. Rev. Lett. **113**, 237202 (2014).

[58] G. H. Wannier, Phys. Rev. **79**, 357 (1950); R. Houtappel, Physica **16**, 425 (1950).

[59] I. Rousochatzakis and N. B. Perkins, In preparation.

[60] E. K.-H. Lee and Y. B. Kim, Phys. Rev. B **91**, 064407 (2015).

[61] D. J. Klein, The Journal of Chemical Physics **61**, 786 (1974).